Published in final edited form as:
Cancer Cell. 2009 June 2; 15(6): 465–476. doi:10.1016/j.ccr.2009.04.011.

Genetic *p53* deficiency partially rescues the adrenocortical dysplasia (*acd*) phenotype at the expense of increased tumorigenesis

Tobias Else[1,*], **Alessia Trovato**[1], **Alex C. Kim**[1], **Yipin Wu**[2], **David O. Ferguson**[2], **Rork D. Kuick**[3], **Peter C. Lucas**[2], and **Gary D. Hammer**[1,*]

1 *Metabolism Endocrinology and Diabetes, Department of Internal Medicine, University of Michigan Health System, Ann Arbor, Michigan, USA*

2 *Department of Pathology, University of Michigan Health System, Ann Arbor, Michigan, USA*

3 *Biostatistics Core of the Cancer Center, University of Michigan Health System, Ann Arbor, Michigan, USA*

Summary

Telomere dysfunction and shortening induce chromosomal instability and tumorigenesis. In this study, we analyze the adrenocortical dysplasia (*acd*) mouse, harboring a mutation in *Tpp1*/*Acd*. Additional loss of *p53* dramatically rescues the *acd* phenotype in an organ-specific manner, including skin hyperpigmentation and adrenal morphology, but not germ cell atrophy. Survival to weaning age is significantly increased in $Acd^{acd/acd}$ $p53^{-/-}$ mice. On the contrary $p53^{-/-}$ and $p53^{+/-}$ mice with the $Acd^{acd/acd}$ genotype show a decreased tumor free survival compared to $Acd^{+/+}$ mice. Tumors from $Acd^{acd/acd}$ $p53^{+/-}$ mice show a striking switch from the classical spectrum of $p53^{-/-}$ mice towards carcinomas. The *acd* mouse model provides further support for an *in vivo* role of telomere deprotection in tumorigenesis.

Significance—Critically shortened dysfunctional telomeres of the $Terc^{-/-}$ mice have been shown to impact tissue development and maintenance and lead to the occurrence of a pro-cancer genome. The present study examines the contribution of telomere shortening vs. telomere deprotection to the development of genetic instability and cancer. By studying the *acd* mouse, we show that telomere deprotection without significant telomere shortening is sufficient to induce tumor formation in the context of p53 absence. It also raises the possibility that telomere deprotection contributes to the high prevalence of carcinomas in humans.

Introduction

Telomere dysfunction has been shown to interfere with tissue maintenance and to induce chromosomal rearrangements which can provide the genetic basis for malignant transformation (Artandi, 2002; Blasco, 2005).

*Corresponding authors: T.E., Department of Internal Medicine - Metabolism, Endocrinology & Diabetes, Molecular Mechanisms of Disease, University of Michigan, 1860 BSRB, 109 Zina Pitcher Pl, Ann Arbor, MI 48109-2200, phone +734 615 8914, fax +734 615-4356. G.D.H., Department of Internal Medicine - Metabolism, Endocrinology & Diabetes, Department of Molecular & Integrative Physiology, Molecular Mechanisms of Disease, BSRB 1502, 109 Zina Pitcher Place, Ann Arbor, Michigan 48109-2200, phone +734 615-2421, fax +734 615-4356.

Telomeres, the outer ends of chromosomes, consist of stretches of hexameric repeats. Over multiple cell cycles telomeres are shortened due to the inability of the semi-conservative DNA replication to completely synthesize the 3′ end of linear chromosomes, which is also known as the end-replication problem. In some tissues and cancers, this problem is overcome by the activity of telomerase, a ribonucleoprotein that adds telomeric repeats to the 3′ end of the leading strand (reviewed by (Greider, 1996)).

Normal telomeres are protected through a specialized DNA structure (T-loop) and a set of protein factors, termed the shelterin complex, which prevents the chromosome ends from causing activation of the DNA damage surveillance and repair machinery, as well as regulating telomerase access (de Lange, 2005). While some parts of the shelterin complex directly bind to either double-stranded (TRF1, TRF2) or single-stranded (POT1) telomere repeats, TIN2, RAP1 and TPP1/ACD serve as critical interconnectors of the shelterin complex. TPP1/ACD (originally termed PTOP, TINT1 and PIP1) was first described as an integral part of the shelterin complex that binds to POT1 and TIN2 (Houghtaling et al., 2004; Liu et al., 2004; Ye et al., 2004). We and others have since shown TPP1/Acd to be necessary for the recruitment of POT1 to the telomere and moreover that it is required for the telomere protective and length regulatory function of POT1 (Hockemeyer et al., 2007; Xin et al., 2007).

Concurrent with the cloning of human *TPP1*/*ACD*, we had identified a recessive mutation (Acd^{acd}) in the mouse ortholog of the gene encoding TPP1 as the genetic cause of the adrenocortical dysplasia (*acd*) phenotype, hence termed *Acd* (Keegan et al., 2005). The *acd* phenotype displays a significant overlap with late generation $Terc^{-/-}$ and $Tert^{-/-}$ mice (Lee et al., 1998; Liu et al., 2000; Rudolph et al., 1999). Both are infertile due to severely reduced spermatogenesis and have a reduced body size. In addition, the *acd* mouse is characterized by skin hyperpigmentation, patchy or absent fur growth, abnormal morphology of the adrenal cortex with large pleomorphic nuclei, skeletal abnormalities and hydronephrosis (Beamer et al., 1994; Keegan et al., 2005).

Most of our current knowledge about the consequences of telomere dysfunction stems from analysis of the phenotype of the $Terc^{-/-}$ mouse, which lacks the telomerase RNA component. The phenotype of $Terc^{-/-}$ mice is believed to be due to a progressive shortening of telomeres over consecutive generations of $Terc^{-/-}$ homozygous breedings and over the lifetime of the $Terc^{-/-}$ organism (Blasco et al., 1997; Chin et al., 1999; Hande et al., 1999; Rudolph et al., 1999). With continued telomere shortening, cells from $Terc^{-/-}$ mice exhibit cytogenetic abnormalities, including chromosomal fusions, presumably due to the ligation of unprotected telomeres by the DNA repair machinery. Similar observations have been made in cell culture models of telomere deprotection such as overexpression of a dominant negative isoform of TRF2 (van Steensel et al., 1998).

In contrast, the *acd* phenotype manifests within the first generation of $Acd^{acd/acd}$ mice generated by heterozygous matings (Beamer et al., 1994; Keegan et al., 2005). The telomere deprotection phenotype in cells lacking *TPP1*/*Acd* has been well described. The acute reduction of TPP1 levels in human cells induces telomere dysfunction-induced foci (TIFs) and telomere elongation (Guo et al., 2007; Hockemeyer et al., 2007; Liu et al., 2004; Ye et al., 2004). Mouse embryo fibroblasts (MEFs) from *acd* mice with a severe deficiency of Tpp1/Acd show a telomere deprotection phenotype and a moderate increase in genomic alterations such as chromosome fusions (Else et al., 2007; Hockemeyer et al., 2007). The acute loss of Tpp1/Acd in *wt* MEFs strongly induces a DNA damage response inducing senescence through a p53-sensitive pathway (Guo et al., 2007; Hockemeyer et al., 2007; Xin et al., 2007).

Telomere dysfunction of $Terc^{-/-}$ mice leads to the accumulation of genomic alterations and the development of tumors (Chin et al., 1999). Cells harboring critically short telomeres are

usually removed from the pool of proliferating cells by p53-dependent pathways leading to apoptosis or senescence in mice and/or additional p16/Ink4a-sensitive pathways in humans (Jacobs and de Lange, 2004; Smogorzewska and de Lange, 2002). In accordance with this finding, *Terc*$^{-/-}$ *p53*$^{-/-}$ exhibit a partial reversal of their infertility due to germ cell failure at the expense of an increased tumor incidence (Artandi et al., 2000; Chin et al., 1999).

With the exception of the *Pot1b*$^{-/-}$ mouse, attempts to create deletions of components of the shelterin complex in whole murine organisms have led to phenotypes with early embryonic lethality (Celli and de Lange, 2005; Chiang et al., 2004; Hockemeyer et al., 2006; Karlseder et al., 2003; Wu et al., 2006). The *Acd*$^{acd/acd}$ genotype that results in a viable mouse despite severe Tpp1/Acd deficiency presents a unique opportunity to investigate the *in vivo* effects of direct telomere deprotection without telomere shortening (Else et al., 2007; Hockemeyer et al., 2007). In order to study the *in vivo* consequences of telomere dysfunction in the absence of telomere shortening, we crossed *Acd*$^{acd/acd}$ mice to a *p53*$^{-/-}$ background and analyzed the surviving offspring for both the rescue of organ phenotypes and the emergence of cancer.

Results

Organ specific rescue of the *acd* phenotype by *p53* ablation

Because the *acd* phenotype is predicted to be induced by telomere dysfunction resulting in activation of p53-sensitive signaling pathways, we crossed *Acd*$^{acd/acd}$ mice to a p53$^{-/-}$ background. On macroscopic examination, a striking complete normalization of the characteristic *acd* phenotype of patchy or complete lack of fur and hyperpigmentation was evident in *Acd*$^{acd/acd}$ *p53*$^{-/-}$ mice (Fig. 1A, Suppl. Fig. 1A). Although the fur and skin phenotype of *acd* mice varied significantly between individual animals, hyperpigmentation in *acd* mice is always present in the skin overlying the paw pads, ears, tail and the ano-genital region. In *Acd*$^{acd/acd}$ *p53*$^{-/-}$ mice, macroscopic hyperpigmentation was completely abolished and there was a dramatic reduction of pigment in epidermis and dermis (Fig. 1B, Suppl. Fig. 1B). Hyperpigmentation in *acd* mice not only led to a darker skin color but was also evident in skin associated lymph nodes presumably due to the uptake and lymphatic transport by macrophages (Suppl. Fig. 4). These dark lymph nodes were not present in *Acd*$^{acd/acd}$ *p53*$^{-/-}$ mice (data not shown).

We analyzed the genotype of 162 male pups resulting from double heterozygous matings (*Acd*$^{+/acd}$ *p53*$^{+/-}$ x *Acd*$^{+/acd}$ *p53*$^{+/-}$) at weaning age (21 days). For *p53*$^{+/+}$ as well as *p53*$^{+/-}$ offspring, a significantly lower number of *Acd*$^{acd/acd}$ genotypes were observed than were expected (p=0.03 and p=0.03, Chi-square test), whereas for *p53*$^{-/-}$ offspring, the *Acd*$^{acd/acd}$ genotypes were nearly in the expected Mendelian proportions (p=0.6), indicating that *p53*$^{-/-}$ increases survival of the *Acd*$^{acd/acd}$ genotype (Fig. 1C). Like *Acd*$^{acd/acd}$ *p53*$^{+/+}$, *Acd*$^{acd/acd}$ *p53*$^{-/-}$ mice were significantly smaller than their respective *Acd*$^{+/+}$ littermates at weaning age (3 weeks) and at 6 weeks of age ($p<10^{-7}$) (Fig. 1D).

Testes of both, *Acd*$^{acd/acd}$ and late generation *Terc*$^{-/-}$ mice, show similar germ cell failure (Hemann et al., 2001; Keegan et al., 2005; Lee et al., 1998). Therefore we examined whether the observed spermatogenic defect involved p53 signaling. In contrast to the observation of a moderate genetic rescue of spermatogenesis in *Terc*$^{-/-}$ *p53*$^{-/-}$ mice and the striking rescue of the skin phenotype in *Acd*$^{acd/acd}$ *p53*$^{-/-}$, we did not find any rescue of the testicular *acd* phenotype in *Acd*$^{acd/acd}$ *p53*$^{-/-}$ mice (Fig. 2A) (Chin et al., 1999). Testes of *Acd*$^{acd/acd}$ mice of all *p53* genotypes either completely lacked (Fig. 2B) or displayed severely reduced spermatogenesis (Fig. 2A) with testis histology reminiscent of a Sertoli cell-only syndrome (SCOS). Total absence of germ cells in tubules without spermatogenesis was confirmed by Gcna immunohistochemistry (Fig. 2A) (Enders and May, 1994). However, in some animals we observed areas of seminiferous tubules with normal spermatogenesis adjacent to empty

seminiferous tubules, completely devoid of germ cells. Relative testicular weights were lower in $Acd^{acd/acd}$ animals regardless of their genetic *p53* status when compared to their $Acd^{+/+}$ littermates (Fig. 2C). Due to the infertility phenotype, male and female mice were regularly housed together and only on very rare occasions did we observe successful pregnancies. Because some components of the adult testis, specifically the Leydig cells, share a common developmental lineage and steroidogenic function with adrenocortical cells, we next examined morphology and characteristics of these interstitial testicular cells (Else and Hammer, 2005). The Leydig and Sertoli cell populations were morphologically normal as evidenced by histologic analysis and Sf1 staining, a marker specific for these cell populations in the testis (Fig. 2A) (Luo et al., 1995). The data indicate that, unlike the spermatogenic defect in $Terc^{-/-}$ mice, the germ cell failure of $Acd^{acd/acd}$ mice may not be caused by p53-mediated senescence or apoptosis and suggests that the $Acd^{acd/acd}$ decapping phenotype may not be identical to a short telomere phenotype or may be of a different degree of severity.

Absence of *p53* partially normalizes the adrenocortical phenotype

The main feature of the *acd* phenotype which led to its name, is the characteristic dysmorphic small adrenal cortex (Beamer et al., 1994). In *acd* adrenal glands there was variable intermingling of the normally distinct adrenal cortex and adrenal medulla, and a lack of the physiological concentric zonation of the mammalian adrenal cortex. Adrenocortical cells of *acd* animals displayed large eosinophilic cytoplasm and prominent enlarged pleomorphic nuclei sometimes harboring inclusion bodies. Remarkably, relative adrenal organ size was completely rescued in $Acd^{acd/acd}$ $p53^{-/-}$ mice and an obvious albeit partial normalization of organ architecture with areas of a distinct cortical zonation was observed (Fig. 3A & 3B). Moreover, while some areas of nuclear atypia remained, $Acd^{acd/acd}$ $p53^{-/-}$ adrenal cortices exhibited a partial rescue in cellular and nuclear size as well (Fig. 3A).

As telomere dysfunction in general and loss of *Tpp1*/*Acd* in particular is known to activate p53 signaling leading to cellular senescence, we examined whether p53-mediated cellular senescence contributed to the adrenal phenotype observed in $Acd^{acd/acd}$ mice. While many adrenocortical cells in $Acd^{acd/acd}$ $p53^{+/+}$ mice stained positive for senescence associated β-galactosidase, a reduced number of stained cells was observed in $Acd^{acd/acd}$ $p53^{-/-}$ adrenal cortices (Suppl. Fig. 2). Consistent with this observation was a reduction of *p21* gene expression (as determined by quantitative RT-PCR analysis) and a reduction in p21 protein (as determined by immunohistochemical analysis) in whole adrenal glands of $Acd^{acd/acd}$ $p53^{-/-}$ mice in comparison to $Acd^{acd/acd}$ $p53^{+/+}$ mice (Fig. 3A & 3C). Caspase 3 and TUNEL staining was typically only observed in $Acd^{+/+}$ $p53^{+/+}$ mice at the corticomedullary boundary, where physiologic apoptosis normally occurs (data not shown). Specifically, there was no increase in cell number or intensity of cells that were positive for apoptotic markers in $Acd^{acd/acd}$ cortices. The changes in senescence associated β-galactosidase activity and in *p21* expression levels as well as the absence of positive markers of apoptosis strongly argue for p53-dependent senescence induction as a main mechanism leading to the adrenocortical phenotype of $Acd^{acd/acd}$ $p53^{+/+}$ mice.

The $Acd^{acd/acd}$ genotype accelerates tumorigenisis in $p53^{-/-}$ mice

In $Terc^{-/-}$ mice, tumors can be observed at old age even without additional genetic challenge. Although we followed a relatively small cohort (5 animals) of $Acd^{acd/acd}$ $p53^{+/+}$, we never observed tumors in either this specific aging cohort or in any other animal of this genotype in our colony (survival 386±78 days, average mean±SD). The cause of death could not be determined in these mice, but the majority suffered from severe uni- or bilateral hydronephrosis (Suppl. Fig. 3). Therefore, to investigate whether the accumulation of genomic alterations leads to increased tumorigenesis a set of four animal groups with the $p53^{-/-}$ or $p53^{+/-}$ genotype and either $Acd^{acd/acd}$ or $Acd^{+/+}$ were analyzed for tumor development. Tumor free survival of

Acd$^{acd/acd}$ *p53*$^{-/-}$ mice was approximately half of that observed in *Acd*$^{+/+}$ *p53*$^{-/-}$ mice ($p=2\times10^{-11}$) (Fig. 4A). Macroscopic and histomorphological analysis of both genotypes identified a tumor spectrum comparable to previous studies of *p53*$^{-/-}$ and *Terc* $^{-/-}$ *p53*$^{-/-}$ mice. Most of the neoplastic lesions belonged to the lymphoma (46% in *Acd*$^{+/+}$ *p53*$^{-/-}$, 38% in *Acd*$^{acd/acd}$ *p53*$^{-/-}$) or sarcoma (44% in *Acd*$^{+/+}$ *p53*$^{-/-}$, 47% in *Acd*$^{acd/acd}$ *p53*$^{-/-}$) spectrum (Fig. 4B, Table 1, Suppl. Fig. 4) (Donehower et al., 1992; Jacks et al., 1994). A sub-analysis of tumor types of the sarcoma spectrum revealed angiosarcomas as the dominant tumor type in both groups followed by undifferentiated sarcomas and rhabdomyosarcomas in *Acd*$^{acd/acd}$ *p53*$^{-/-}$ mice and fibrosarcomas in *Acd*$^{+/+}$ *p53*$^{-/-}$ mice. Interestingly, two tumors (6%) of the carcinoma spectrum were observed in the *Acd*$^{acd/acd}$ *p53*$^{-/-}$ but none in the *Acd*$^{+/+}$ *p53*$^{-/-}$ group (Table 1).

Acd$^{acd/acd}$ *p53*$^{+/-}$ mice predominantly develop tumors of the carcinoma spectrum

As in the *p53*$^{-/-}$ groups, tumor risk was approximately doubled in *Acd*$^{acd/acd}$ *p53*$^{+/-}$ compared to *Acd*$^{+/+}$ *p53*$^{+/-}$ mice ($p=2\times10^{-9}$) (Fig. 4A). Paralleling the reports for *Terc*$^{-/-}$ mice, we observed a remarkable difference in histological tumor types between these animal groups (Artandi et al., 2000). The main tumor type observed in *Acd*$^{+/+}$ *p53*$^{+/-}$ mice was sarcoma, with a preponderance of osteosarcomas. However the majority of neoplasms in *Acd*$^{acd/acd}$ *p53*$^{+/-}$ animals were carcinomas, varying from squamous cell carcinomas (SCC) to adenocarcinomas with a large fraction exhibiting adenosquamous differentiation (Fig. 4C, Fig. 5A, Table 1). The majority of these tumors identified by routine histological analyses also stained positive for pankeratin confirming the diagnosis of carcinoma-type tumors (Fig. 5A). Most carcinomas grew as subcutaneous lesions attached to the cutis and frequently presented with ulcerations, suggestive of an epidermal origin (Fig. 5B). While some of the SCCs appeared to directly arise from the epidermis, the adeno- and adenosquamous carcinomas may have their origin in epidermis-associated glands such as sweat or mammary glands. Most interestingly, 5% of tumors were of adrenocortical origin as proven by positive Sf1 staining (Fig. 5C, Fig. 5D, Table 1). None of these adrenocortical cancers (ACC) stained positive for p21 (Fig. 5C) as shown for the normal *acd* adrenal cortex (Fig. 3A). This is further evidence that these tumor cells bypassed the senescent phenotype at some point in the process of neoplastic transformation. Finally, at least 11 of 16 tumors from *Acd*$^{acd/acd}$ *p53*$^{+/-}$ mice showed apparent loss of the *wt p53* allele, whereas at most 4 of 14 tumors from *Acd*$^{+/+}$ *p53*$^{+/-}$ mice showed a similar loss (Suppl. Fig. 5).

Genomic alterations underlying tumorigenesis in *Acd*$^{acd/acd}$ mice are the consequence of dysfunctional telomeres and subsequent breakage fusion bridge cycles

Cells derived from *Acd*$^{acd/acd}$ animals display deprotected telomeres and acquire genomic aberrations (Else et al., 2007; Hockemeyer et al., 2007). Tumors from *Acd*$^{acd/acd}$ *p53*$^{-/-}$ showed a significant higher number of TIFs (Fig. 6A, Fig. 6B). As further evidence for dysfunctional telomeres as the underlying mechanism of tumorigenesis, we observed a significantly higher percentage of anaphase bridges in tissue sections from tumors of *Acd*$^{acd/acd}$ animals (Fig. 6C). Some of the mitotic figures with anaphase bridges revealed multiple strings of chromatin spanning the two poles of the dividing cells and in some cases, genomic material seemed to be localized or trapped between the two dividing poles, lacking a clear connection to either side (Fig. 6D).

We next compared telomere length in neoplastic and non-neoplastic tissues from different genotypes. In contrast to previous cell culture experiments that reported an increase in telomere length we did not observe a significant difference between non-neoplastic tissues from *Acd*$^{acd/acd}$ and *Acd*$^{+/+}$ animals (Fig. 6E). Some degree of telomere shortening was observed in some tumors when compared to non-neoplastic tissue regardless whether they were from *Acd*$^{acd/acd}$ or *Acd*$^{+/+}$ animals. This is in contrast to the Terc$^{-/-}$ mouse model where progressive

telomere shortening provides the basis for telomere dysfunction. Anaphase bridges are viewed as one morphological correlate of breakage-fusion bridge cycles (BFBs). Therefore, we analyzed tumors and a tumor cell line by comparative genomic hybridization (CGH) and spectral karyotyping respectively. In CGH analysis multiple amplifications as well as areas of "step-like" amplifications were present in the genome from $Acd^{acd/acd}$ tumors (Fig. 7A & 7B, Suppl. Fig. 6). These alterations are an expected result of recurrent BFBs. The average number of segments deviating from the normal tissue baseline was higher in $Acd^{acd/acd}$ than $Acd^{+/+}$ tumors (90.6 +/− 38.4 transition points vs. 27 +/− 8.3 transition points, p=0.0048) (Fig. 7A). As this analysis may be influenced by simple background noise of the hybridization analysis, we next identified the number of chromosomes affected by copy number alterations. There were significantly more chromosomes with at least one copy number change in $Acd^{acd/acd}$ than $Acd^{+/+}$ tumors. Notably, several of the observed amplifications encompass loci that may contribute to tumorigenesis. This includes amplifications of potential or proven oncogenes such as the cluster of *Wnt* genes on chromosome 11 and the *Kras* locus on chromosome 6, which has recently been shown to be amplified in tumors from $Terc^{-/-}$ mice. As a proof of principle, we found very specific rearrangements by spectral karyotyping analysis of an $Acd^{acd/acd}$ $p53^{-/-}$ rhabdomyosarcoma cell line, consisting of segments of two different chromosomes in an alternating pattern (Fig. 7C). These alterations are likely due to reoccurring BFBs involving two different chromosomes and represent the cytogenetic correlate of the stepwise regional amplifications found in CGH analysis.

Discussion

In this study we show that the ablation of *p53* both profoundly rescues a number of characteristics of the *acd* phenotype and increases tumorigenesis. These results underscore the importance of p53 activation as a driving force in the development of major characteristics of the adrenocortical dysplasia phenotype. The *acd* mouse is the first viable animal model that permits analysis of the selective deficiency of an integral part of the shelterin complex. Moreover, *acd* mice allow for analysis of the contribution of telomere deprotection in the absence of telomere shortening to genetic instability and tumorigenesis. In contrast telomere dysfunction in $Terc^{-/-}$ mice is less defined and only observed after significant telomere shortening following breeding over successive generations. Deprotection versus shortening may underlie the distinct phenotypes of *acd* mice and $Terc^{-/-}$ mice.

Phenotypic rescue through the ablation of *p53* in the $Acd^{acd/acd}$ mice was most profound in the skin where hyperpigmention was macroscopically completely absent in $Acd^{acd/acd}$ $p53^{-/-}$ mice. Two possible scenarios are discussed as the basis for hyperpigmentation in *acd* mice. Elevated ACTH and MSH levels in the setting of adrenocortical insufficiency could directly stimulate melanocytes or, alternatively, melanocytes that progressed to senescence could be more active in terms of pigment production. The first possibility seems to be unlikely because mouse models of adrenocortical insufficiency like the $Mc2r^{-/-}$ (ACTH receptor) mouse do not develop hyperpigmentation (personal communication D. Chida) (Chida et al., 2007). Furthermore, we were not able to detect significant differences in baseline ACTH and corticosterone levels (data not shown). Overall it seems more likely that skin hyperpigmentation is induced by telomere deprotection and direct activation of p53-sensitive pathways in melanocytes as it has been shown for other mouse models (Atoyan et al., 2007; Cui et al., 2007; Hadshiew et al., 2008; Khlgatian et al., 2002).

Male germ cells have a very high proliferative rate and therefore, seem to depend more than other tissues on telomere integrity and perhaps telomerase activity (Hemann et al., 2001; Lee et al., 1998). We did not observe any rescue of the testicular $Acd^{acd/acd}$ phenotype through *p53* ablation in $Acd^{acd/acd}$ animals, which is in contrast to the moderate rescue observed in late generation $Terc^{-/-}$ $p53^{-/-}$ mice (Chin et al., 1999). Therefore, it can be hypothesized that unlike

other tissues, germ cells do not completely depend on p53-sensitive pathways to induce their removal from the proliferative cell pool. It is also possible that different degrees of severity of telomere dysfunction can induce alternative pathways in an organ-dependent manner. The observation of completely empty SCOS-like tubules adjacent to seminiferous tubules with grossly normal spermatogenesis suggests a developmental defect in $Acd^{acd/acd}$ mice, as it seems unlikely that the complete germ cell epithelium of some tubules but not others disappears at the same time as the result of postnatal germ cell failure. For a degenerative mechanism in adult life, one would expect random losses of germ cells and an overall reduction of spermatogenesis rather than the observed “all-or-nothing” phenomenon. It is worthwhile mentioning that *TPP1*/*ACD* expression and telomerase activity are reduced in biopsies of SCOS testes (Feig et al., 2007; Schrader et al., 2002).

A main characteristic of the *acd* phenotype is cytomegalic adrenal hypolplasia congenita (AHC) which is not observed in late generation $Terc^{-/-}$ mice (data not shown) and has not been reported for any other mouse model of telomere dysfunction. In this study we show that the adrenal *acd* phenotype is caused by the induction of p53-dependent senescence. In the adrenal cortex of $Acd^{acd/acd}$ $p53^{-/-}$ mice we observe a normalization of organ size and architecture. In humans, cytomegalic AHC is observed in random pediatric or fetal autopsies as well as part of several syndromes. The majority of humans with cytomegalic AHC (with hypogonadotropic hypogonadism) have a germ line mutation in *NR0B1* (*DAX1*) (Achermann et al., 1999; Zanaria et al., 1994). The emerging role of NR0B1 in embryonic and tumor stem cell physiology suggests that cytomegalic adrenal failure may reflect a common morphological endpoint of stem cell failure and exhaustion of organ maintenance capacity due to a number of causes, including telomere dysfunction (Kim et al., 2008; Mendiola et al., 2006; Niakan et al., 2006).

In summary, ablation of *p53* rescues the $Acd^{acd/acd}$ phenotype to varying degrees and in an organ-specific manner. The differences of the $Acd^{acd/acd}$ and the $Terc^{-/-}$ phenotype and their different rescue by *p53* ablation can be explained by distinct molecular mechanisms induced by either short telomeres or deprotected telomeres. Alternatively, telomere dysfunction induced by deprotection in $Acd^{acd/acd}$ mice could be more severe than telomere dysfunction induced by telomere shortening in $Terc^{-/-}$ mice and therefore not as readily rescued by simple *p53* ablation. Indeed, one would expect some telomere deprotection on every telomere in $Acd^{acd/acd}$ mice due to the severe deficiency in Tpp1/Acd as opposed to $Terc^{-/-}$ mice, where telomere decapping gradually develops with the loss of telomere sequences, resulting in the inability to bind shelterin components. Furthermore, it would be of interest to investigate potential roles of TPP1/Acd independent of its function in telomere protection. Such functions have been discovered for the protein component of telomerase TERT that participates in telomere-independent stem cell physiology (Choi et al., 2008; Sarin et al., 2005).

The onset of tumor development was significantly accelerated in $Acd^{acd/acd}$ $p53^{-/-}$ and $Acd^{acd/acd}$ $p53^{+/-}$ mice when compared to their $Acd^{+/+}$ $p53^{-/-}$ *and* $Acd^{+/+}$ $p53^{+/-}$ littermates, respectively. This underscores the role of telomere dysfunction in the induction of tumorigenesis as it has been described for $Terc^{-/-}$ mice (Artandi et al., 2000; Chin et al., 1999). For the $Acd^{acd/acd}$ phenotype, the sole driving force for genomic instability can be attributed to the telomere deprotection phenotype (Else et al., 2007; Hockemeyer et al., 2007). In contrast to the $Terc^{-/-}$ mice, no telomere shortening was necessary for tumor development. Though our experiments do not entirely exclude the possibility that a small fraction of telomeres reach a critical short length and dysfunctional state, this possibility seems to be unlikely as we did not observe any differences in telomere length comparing normal tissues from $Acd^{acd/acd}$ and $Acd^{+/+}$ animals. Some degree of telomere shortening was inconsistently observed comparing tumor tissue and normal tissue (liver) from the same animal and was independent of the *Acd* genotype. Furthermore, a hallmark of telomere dysfunction

in *Terc*$^{-/-}$ mice is the presence of chromosomal fusions lacking telomere signals at the fusion site (Hande et al., 1999). In contrast, we have previously shown that telomere signals are detectable at the non-homologous fusion sites in *Acd*$^{acd/acd}$ MEFs (Else et al., 2007). The lack of significant telomere length differences between *Acd*$^{acd/acd}$ and *Acd*$^{+/+}$ animals shows that *Tpp1*/*Acd* deficiency *in vivo* does not lead to average telomere length differences as opposed to reports in human cells where the acute loss of *TPP1*/*ACD*, or the use of a dominant negative isoform, leads to excessive telomere lengthening (O'Connor et al., 2006; Xin et al., 2007; Ye et al., 2004).

Considering the role of telomeres and telomerase in the telomere-based two step model of carcinogenesis, the *acd* mouse is a useful tool to selectively investigate the *in vivo* consequences of telomere deprotection (Artandi and DePinho, 2000; Cosme-Blanco et al., 2007; Ju and Rudolph, 2006). Telomere dysfunction is hypothesized to lead to genomic shuffling via BFBs, which contributes to tumorigenesis. Later, the genome becomes stabilized through a telomere maintenance mechanism such as telomerase activity or alternative telomere length maintenance mechanisms (ALT) (Farazi et al., 2003; Maser and DePinho, 2002; Rudolph et al., 2001). Telomere deprotection has been recently suggested to participate in oncogenesis in a variety of human cancers (Poncet et al., 2008; Vega et al., 2008). Our studies of the *Acd*$^{acd/acd}$ *p53*$^{-/-}$ mouse model reproduce the genomic alterations proposed by the telomere-based model of carcinogenesis (Chin et al., 2004; O'Hagan et al., 2002). The multiple chromosomal amplifications and cytogenic changes observed in *Acd*$^{acd/acd}$ tumors together with an increased number of anaphase bridges support BFBs as a main mechanism of ongoing genomic alterations in tumorigenesis. Additionally, we argue that BFB-induced losses of genetic material are also responsible for the increased frequency of loss of the *wt p53* allele in *Acd*$^{acd/acd}$ *p53*$^{+/-}$ vs. *Acd*$^{+/+}$ *p53*$^{+/-}$ tumors.

The observations of marked senescence in the adrenal cortex of *Acd*$^{acd/acd}$ mice and the development of ACC in *Acd*$^{acd/acd}$ *p53*$^{+/-}$ mice, suggests that the escape from senescence may contribute to adrenocortical carcinogenesis. Although ACC is not the main neoplasia (5% of tumors in *Acd*$^{acd/acd}$ *p53*$^{+/-}$) observed in this study, it is a finding of great importance as there is currently no mouse model that specifically develops ACCs. ACC in humans is a rare disease with a dismal prognosis. Mouse models of telomere dysfunction may be further exploited to study this rare type of cancer and may serve as a useful tool to understand the pathogenesis and pathophysiology of this disease. In humans ACC is one of the syndrome-defining pathologies in Li-Fraumeni syndrome. The specific occurrence of this tumor in *Acd*$^{acd/acd}$ *p53*$^{+/-}$ mice may further suggest a participation of telomere dysfunction in Li-Fraumeni associated carcinogenesis. Indeed it has recently been shown that telomere length correlates with age at tumor onset in patients with Li-Fraumeni (Tabori et al., 2007).

It has been assumed for a long time that telomere deprotection can provide the basis for generating a pro-cancer genome during tumorigenesis in human tissues. We believe that the *acd* mouse provides an excellent model for the *in vivo* dissection of these mechanisms underlying this phenomenon and will increase our understanding of how telomere pathophysiology impacts the origin of tumors in mammalian organisms. Lastly *TPP1*/*ACD* and other genes of the shelterin complex may facilitate both our understanding of a genetic basis in patients with dyskeratosis congenital-like heritable cancer syndromes that do not exhibit significant changes in overall telomere length.

Experimental procedures

Animal procedures

All experiments involving animals were performed in accordance with institutionally approved and current animal care guidelines (UCUCA-09458). Adrenocortical dysplasia (*acd*) mice used

in this study were from a mixed DW/JxCAST/Ei background and genotyped as described previously (Keegan et al., 2005). *p53*$^{-/-}$ mice (C57BL6/J;*Trp53*^{tm1Tyj}) were purchased from Jackson Laboratories (JAX mice and Services, Bar Harbor, ME) and genotyped as described previously (Jacks et al., 1994). Double heterozygous animals (*Acd*$^{+/acd}$ *p53*$^{+/-}$) were crossed to generate the genotypes used in this study. A series of animals (≥5) of each genotype were weighed at 3 weeks and 6 weeks. Initially autopsies were conducted at 6 weeks of age, when organ weights of adrenal glands and testis were recorded and tissues were either preserved for histological analysis or snap frozen for RNA preparation. For survival studies autopsy was conducted either at the time of obvious tumor growth or at spontaneous death. Some tumors samples were used to establish cell lines. Parts of the tumor were disintegrated using cell strainers, washed in PBS and grown on fibronectin (Sigma, St. Louis, MO) coated plates in DMEM supplemented with 5% FBS and antifungal, antibacterial solution (all Invitrogen, Carlsbad, CA). Chi-Square test was used to test the amount of observed pups with the *Acd*$^{acd/acd}$ genotype within a certain *p53* genotype. Survival between groups was analyzed with log-rank tests. Animals without obvious tumor, or in which degradation precluded meaningful analysis or with a histological benign pathology were considered censored at the time of death.

Histology and Immunohistochemistry

For general histological analysis tissues were fixed in 4% formaldehyde, dehydrated and paraffin embedded. 6μm sections were used for routine hematoxylin and eosin staining or further immunohistological procedures. Immunohistochemical analyses followed standard protocols using the ABC Elite kit (Vector Laboratories, Burlingame, CA) and DAB Sigma Fast (Sigma, St. Louis, MO) or fluorescent secondary antibodies. Primary antibody incubation was done at 4°C overnight. Primary and secondary antibodies were used at the following concentrations: p21 (1:50, mouse monoclonal, #556430, BD Biosciences, San Jose, CA), GCNA (1:200, rat monoclonal IgM, obtained from G. C. Enders (Enders and May, 1994)), Sf1 (1:1000, provided by Ken-ichirou Morohashi), pan-keratin (1:100, mouse monoclonal, #MS343, Lab Vision, Fremont, CA), γH2ax (1:50, #2577 Cell Signalling, Danvers, MA), biotinylated anti-mouse (1:200, BA9200, Vector Laboratories, Burlingame, CA), biotinylated anti-rabbit (1:200, BA1000, Vector Laboratories, Burlingame, CA), biotinylated-anti-rat (1:200, #161603, KPL, Gaithersburg, MD), Alexa-Fluor 486-coupled anti mouse IgG (1:200, #A11029, Carlsbad, CA),. Telomere FISH procedure was conducted as described previously following a protocol modified from Meeker et al. (Else et al., 2008; Meeker et al., 2002). Pictures were taken and in plane telomere signals were counted (at least 250/slide) in nuclei with positive γH2ax staining. The ratio of telomeres with to telomeres without co-localizing γH2ax staining (TIFs) was calculated for at least 4 tumors per group. Anaphase bridges and anaphase mitoses were counted in ≥4 tumors per genotype. The anaphase bridge index was calculated as the ratio of anaphase bridges per total metaphases. Pathological diagnosis was made in synopsis of macroscopic and microscopic pathologies. Images were captured with an Optiphot-2 microscope (Nikon, Melville, NY) with a DP-70 camera and software system (Olympus, Hauppauge, NY). For comparative immunohistochemical analyses, system and software processing (Adobe Photoshop, Adobe Illustrator, San Jose, CA) settings were kept constant over sample groups. For statistical analysis data were fit using a 1-way ANOVA, and pairs of groups compared using the resulting F-tests.

Reverse Transcribed Quantitative Polymerase Chain Reaction (RT-qPCR)

RNA was extracted from adrenal glands by a standard method using TRIzol® (Invitrogen, Carlsbad, CA). RNA was quantified and reverse transcription was carried out using the i-Script™ kit (Bio-Rad, Hercules, CA) following the manufacturers protocol. Intron spanning primers were used for Gapdh (fwd, 5′-TGT CCG TCG TGG ATC TGA C-3′; rev, 5-CCT GCT TCA CCA CCT TCT TG-3′), Sf1 (fwd, 5′-ACA AGC ATT ACA CGT GCA CC-3′; rev, 5′-

TGA CTA GCA ACC ACC TTG CC-3′), p21 (Cdkn1a) (fwd 5′-TCC ACA GCG ATA TCC AGA CA-3′; rev, 5′-GGA CAT CAC CAG GAT TGG AC-3′) (Invitrogen, Carlsbad, CA). For the PCR reaction 2x SYBR Green PCR master mix was used in a ABI 7300 thermocycler (both Applied Biosystems, Foster City, CA). For statistical analysis data were fit using a 1-way ANOVA, and pairs of groups compared using F-tests.

Telomere restriction fragment (TRF) length assay

TRF analysis utilized published protocols with modifications (Else et al., 2008; Hemann and Greider, 2000). A purification kit (#13343, Qiagen, Hilden, Germany) was used to obtain high molecular weight genomic DNA. 2μg genomic DNA were digested with 60U of Dpn II for 36h and run in 1% agarose (Seakem, Lonza, Rockland, ME) using a CHEF mapper (BioRad, Hercules, CA). The automatic algorithm was set to a range of 5kb to 200kb. A PFG low molecular weight marker (NEB, Ipswich, MA) was used as a size marker. DNA-gels were further processed as described previously (Else et al., 2008).

Comparative Genomic Hybridization (CGH)

Isolated high molecular weight genomic DNA (#13343, Qiagen, Hilden, Germany) from 6 *acd* tumors and 4 *wt* tumors was run on a 1% agarose gel and spectrophotometric measurements at 230nm, 260nm and 280nm were conducted to exclude samples with significant degradation or contamination. CGH was conducted on the CGH0150-WMG platform using the NimbleGen service (NimbleGen, Madison, WI). The raw data is available in ArrayExpress (experiment E-TABM-680). The NimbleGen CGH-SegMNT algorithm was used to divide chromosomes into segments that were separated by transitions in the logarithm of test to reference sample ratios. We excluded data from the Y chromosome (which had a lower probe density) as well as small segments represented by 30 or fewer probes. The software created segments even when the change in average estimated log-ratio was very small. Consequently we selected segments as abnormal if the base-2 log-ratio was greater than 0.5 or less than −0.5, or if the log-ratio was larger than 0.3 in absolute value and the change in log-ratio from the previous segment was also greater than 0.3. The second criterion selects segments where the change in copy number was abrupt, while the first criterion selects a segment even if the estimated log-ratio rises and falls gradually. We combined neighboring selected segments that were all estimated to have copy numbers greater than 2, or all less than 2, into “runs”, and counted the number of distinct runs in each tumor. We counted the total number of chromosomes containing selected segments for each tumor, and compared these and the other metrics between $Acd^{acd/acd}$ and $Acd^{+/+}$ tumors using one-sided Rank-Sum tests.

Karyotypic Analyses

Metaphases were generated using standard procedures. Slides were then subjected to SKY analysis using mouse SKY paint mixture from Applied Spectral Imaging (ASI, Vista, CA) according to the manufacturer’s protocol. All imaging was performed on an Olympus BX-61 microscope equipped with an interferometer driven by a desktop computer and specialized software (ASI, Vista, CA). Inverted DAPI images were generated using SKYview software (ASI, Vista, CA).

Supplementary Material

Refer to Web version on PubMed Central for supplementary material.

Acknowledgments

TE and AT were sponsored through generous scholarships by the Garry Betty Foundation. This work has been sponsored by grant NIH NIDDK DK62027 (GDH) and a grant from the Sidney Kimmel Cancer Research Foundation

(DOF). The authors would like to thank the DNA sequencing core facility at the University of Michigan, Tom Giordano for his endocrine pathology expertise, Buffy Ellsworth from Sally Camper's Lab for IHC advice and Jose Luis Garcia Perez for intellectual exchange and experimental advice, as well as Guido Bommer, Joanne Heaton, Catherine Keegan and Sonalee Shah for editorial advice.

Literature

Achermann JC, Gu WX, Kotlar TJ, Meeks JJ, Sabacan LP, Seminara SB, Habiby RL, Hindmarsh PC, Bick DP, Sherins RJ, et al. Mutational analysis of DAX1 in patients with hypogonadotropic hypogonadism or pubertal delay. J Clin Endocrinol Metab 1999;84:4497–4500. [PubMed: 10599708]

Artandi SE. Telomere shortening and cell fates in mouse models of neoplasia. Trends Mol Med 2002;8:44–47. [PubMed: 11796266]

Artandi SE, Chang S, Lee SL, Alson S, Gottlieb GJ, Chin L, DePinho RA. Telomere dysfunction promotes non-reciprocal translocations and epithelial cancers in mice. Nature 2000;406:641–645. [PubMed: 10949306]

Artandi SE, DePinho RA. A critical role for telomeres in suppressing and facilitating carcinogenesis. Curr Opin Genet Dev 2000;10:39–46. [PubMed: 10679392]

Atoyan RY, Sharov AA, Eller MS, Sargsyan A, Botchkarev VA, Gilchrest BA. Oligonucleotide treatment increases eumelanogenesis, hair pigmentation and melanocortin-1 receptor expression in the hair follicle. Exp Dermatol 2007;16:671–677. [PubMed: 17620094]

Beamer WG, Sweet HO, Bronson RT, Shire JG, Orth DN, Davisson MT. Adrenocortical dysplasia: a mouse model system for adrenocortical insufficiency. J Endocrinol 1994;141:33–43. [PubMed: 8014601]

Blasco MA. Telomeres and human disease: ageing, cancer and beyond. Nat Rev Genet 2005;6:611–622. [PubMed: 16136653]

Blasco MA, Lee HW, Hande MP, Samper E, Lansdorp PM, DePinho RA, Greider CW. Telomere shortening and tumor formation by mouse cells lacking telomerase RNA. Cell 1997;91:25–34. [PubMed: 9335332]

Celli GB, de Lange T. DNA processing is not required for ATM-mediated telomere damage response after TRF2 deletion. Nat Cell Biol 2005;7:712–718. [PubMed: 15968270]

Chiang YJ, Kim SH, Tessarollo L, Campisi J, Hodes RJ. Telomere-associated protein TIN2 is essential for early embryonic development through a telomerase-independent pathway. Mol Cell Biol 2004;24:6631–6634. [PubMed: 15254230]

Chida D, Nakagawa S, Nagai S, Sagara H, Katsumata H, Imaki T, Suzuki H, Mitani F, Ogishima T, Shimizu C, et al. Melanocortin 2 receptor is required for adrenal gland development, steroidogenesis, and neonatal gluconeogenesis. Proc Natl Acad Sci U S A 2007;104:18205–18210. [PubMed: 17989225]

Chin K, de Solorzano CO, Knowles D, Jones A, Chou W, Rodriguez EG, Kuo WL, Ljung BM, Chew K, Myambo K, et al. In situ analyses of genome instability in breast cancer. Nat Genet 2004;36:984–988. [PubMed: 15300252]

Chin L, Artandi SE, Shen Q, Tam A, Lee SL, Gottlieb GJ, Greider CW, DePinho RA. p53 deficiency rescues the adverse effects of telomere loss and cooperates with telomere dysfunction to accelerate carcinogenesis. Cell 1999;97:527–538. [PubMed: 10338216]

Choi J, Southworth LK, Sarin KY, Venteicher AS, Ma W, Chang W, Cheung P, Jun S, Artandi MK, Shah N, et al. TERT promotes epithelial proliferation through transcriptional control of a Myc- and Wnt-related developmental program. PLoS Genet 2008;4:e10. [PubMed: 18208333]

Cosme-Blanco W, Shen MF, Lazar AJ, Pathak S, Lozano G, Multani AS, Chang S. Telomere dysfunction suppresses spontaneous tumorigenesis in vivo by initiating p53-dependent cellular senescence. EMBO Rep 2007;8:497–503. [PubMed: 17396137]

Cui R, Widlund HR, Feige E, Lin JY, Wilensky DL, Igras VE, D'Orazio J, Fung CY, Schanbacher CF, Granter SR, Fisher DE. Central role of p53 in the suntan response and pathologic hyperpigmentation. Cell 2007;128:853–864. [PubMed: 17350573]

de Lange T. Shelterin: the protein complex that shapes and safeguards human telomeres. Genes Dev 2005;19:2100–2110. [PubMed: 16166375]

Donehower LA, Harvey M, Slagle BL, McArthur MJ, Montgomery CA Jr, Butel JS, Bradley A. Mice deficient for p53 are developmentally normal but susceptible to spontaneous tumours. Nature 1992;356:215–221. [PubMed: 1552940]

Else T, Giordano TJ, Hammer GD. Evaluation of telomere length maintenance mechanisms in adrenocortical carcinoma. J Clin Endocrinol Metab 2008;93:1442–1449. [PubMed: 18198226]

Else T, Hammer GD. Genetic analysis of adrenal absence: agenesis and aplasia. Trends Endocrinol Metab 2005;16:458–468. [PubMed: 16275119]

Else T, Theisen BK, Wu Y, Hutz JE, Keegan CE, Hammer GD, Ferguson DO. Tpp1/Acd maintains genomic stability through a complex role in telomere protection. Chromosome Res 2007;15:1001–1013. [PubMed: 18185984]

Enders GC, May JJ 2nd. Developmentally regulated expression of a mouse germ cell nuclear antigen examined from embryonic day 11 to adult in male and female mice. Dev Biol 1994;163:331–340. [PubMed: 8200475]

Farazi PA, Glickman J, Jiang S, Yu A, Rudolph KL, DePinho RA. Differential impact of telomere dysfunction on initiation and progression of hepatocellular carcinoma. Cancer Res 2003;63:5021–5027. [PubMed: 12941829]

Feig C, Kirchhoff C, Ivell R, Naether O, Schulze W, Spiess AN. A new paradigm for profiling testicular gene expression during normal and disturbed human spermatogenesis. Mol Hum Reprod 2007;13:33–43. [PubMed: 17114209]

Greider CW. Telomere length regulation. Annu Rev Biochem 1996;65:337– 365. [PubMed: 8811183]

Guo X, Deng Y, Lin Y, Cosme-Blanco W, Chan S, He H, Yuan G, Brown EJ, Chang S. Dysfunctional telomeres activate an ATM-ATR-dependent DNA damage response to suppress tumorigenesis. Embo J 2007;26:4709–4719. [PubMed: 17948054]

Hadshiew I, Barre K, Bodo E, Funk W, Paus R. T-oligos as differential modulators of human scalp hair growth and pigmentation: a new "time lapse system" for studying human skin and hair follicle biology in vitro? Arch Dermatol Res 2008;300:155–159. [PubMed: 18239924]

Hande MP, Samper E, Lansdorp P, Blasco MA. Telomere length dynamics and chromosomal instability in cells derived from telomerase null mice. J Cell Biol 1999;144:589–601. [PubMed: 10037783]

Hemann MT, Greider CW. Wild-derived inbred mouse strains have short telomeres. Nucleic Acids Res 2000;28:4474–4478. [PubMed: 11071935]

Hemann MT, Rudolph KL, Strong MA, DePinho RA, Chin L, Greider CW. Telomere dysfunction triggers developmentally regulated germ cell apoptosis. Mol Biol Cell 2001;12:2023–2030. [PubMed: 11452000]

Hockemeyer D, Daniels JP, Takai H, de Lange T. Recent expansion of the telomeric complex in rodents: Two distinct POT1 proteins protect mouse telomeres. Cell 2006;126:63–77. [PubMed: 16839877]

Hockemeyer D, Palm W, Else T, Daniels JP, Takai KK, Ye JZ, Keegan CE, de Lange T, Hammer GD. Telomere protection by mammalian Pot1 requires interaction with Tpp1. Nat Struct Mol Biol 2007;14:754–761. [PubMed: 17632522]

Houghtaling BR, Cuttonaro L, Chang W, Smith S. A dynamic molecular link between the telomere length regulator TRF1 and the chromosome end protector TRF2. Curr Biol 2004;14:1621–1631. [PubMed: 15380063]

Jacks T, Remington L, Williams BO, Schmitt EM, Halachmi S, Bronson RT, Weinberg RA. Tumor spectrum analysis in p53-mutant mice. Curr Biol 1994;4:1–7. [PubMed: 7922305]

Jacobs JJ, de Lange T. Significant role for p16INK4a in p53- independent telomere-directed senescence. Curr Biol 2004;14:2302–2308. [PubMed: 15620660]

Ju Z, Rudolph KL. Telomeres and telomerase in cancer stem cells. Eur J Cancer 2006;42:1197–1203. [PubMed: 16644207]

Karlseder J, Kachatrian L, Takai H, Mercer K, Hingorani S, Jacks T, de Lange T. Targeted deletion reveals an essential function for the telomere length regulator Trf1. Mol Cell Biol 2003;23:6533–6541. [PubMed: 12944479]

Keegan CE, Hutz JE, Else T, Adamska M, Shah SP, Kent AE, Howes JM, Beamer WG, Hammer GD. Urogenital and caudal dysgenesis in adrenocortical dysplasia (acd) mice is caused by a splicing mutation in a novel telomeric regulator. Hum Mol Genet 2005;14:113–123. [PubMed: 15537664]

Khlgatian MK, Hadshiew IM, Asawanonda P, Yaar M, Eller MS, Fujita M, Norris DA, Gilchrest BA. Tyrosinase gene expression is regulated by p53. J Invest Dermatol 2002;118:126–132. [PubMed: 11851885]

Kim J, Chu J, Shen X, Wang J, Orkin SH. An extended transcriptional network for pluripotency of embryonic stem cells. Cell 2008;132:1049–1061. [PubMed: 18358816]

Lee HW, Blasco MA, Gottlieb GJ, Horner JW 2nd, Greider CW, DePinho RA. Essential role of mouse telomerase in highly proliferative organs. Nature 1998;392:569–574. [PubMed: 9560153]

Liu D, Safari A, O'Connor MS, Chan DW, Laegeler A, Qin J, Songyang Z. PTOP interacts with POT1 and regulates its localization to telomeres. Nat Cell Biol 2004;6:673–680. [PubMed: 15181449]

Liu Y, Snow BE, Hande MP, Yeung D, Erdmann NJ, Wakeham A, Itie A, Siderovski DP, Lansdorp PM, Robinson MO, Harrington L. The telomerase reverse transcriptase is limiting and necessary for telomerase function in vivo. Curr Biol 2000;10:1459–1462. [PubMed: 11102810]

Luo X, Ikeda Y, Lala DS, Baity LA, Meade JC, Parker KL. A cell-specific nuclear receptor plays essential roles in adrenal and gonadal development. Endocr Res 1995;21:517–524. [PubMed: 7588417]

Maser RS, DePinho RA. Connecting chromosomes, crisis, and cancer. Science 2002;297:565–569. [PubMed: 12142527]

Meeker AK, Gage WR, Hicks JL, Simon I, Coffman JR, Platz EA, March GE, De Marzo AM. Telomere length assessment in human archival tissues: combined telomere fluorescence in situ hybridization and immunostaining. Am J Pathol 2002;160:1259–1268. [PubMed: 11943711]

Mendiola M, Carrillo J, Garcia E, Lalli E, Hernandez T, de Alava E, Tirode F, Delattre O, Garcia-Miguel P, Lopez-Barea F, et al. The orphan nuclear receptor DAX1 is up-regulated by the EWS/FLI1 oncoprotein and is highly expressed in Ewing tumors. Int J Cancer 2006;118:1381–1389. [PubMed: 16206264]

Niakan KK, Davis EC, Clipsham RC, Jiang M, Dehart DB, Sulik KK, McCabe ER. Novel role for the orphan nuclear receptor Dax1 in embryogenesis, different from steroidogenesis. Mol Genet Metab 2006;88:261–271. [PubMed: 16466956]

O'Connor MS, Safari A, Xin H, Liu D, Songyang Z. A critical role for TPP1 and TIN2 interaction in high-order telomeric complex assembly. Proc Natl Acad Sci U S A 2006;103:11874–11879. [PubMed: 16880378]

O'Hagan RC, Chang S, Maser RS, Mohan R, Artandi SE, Chin L, DePinho RA. Telomere dysfunction provokes regional amplification and deletion in cancer genomes. Cancer Cell 2002;2:149–155. [PubMed: 12204535]

Poncet D, Belleville A, de Roodenbeke CT, de Climens AR, Simon EB, Merle-Beral H, Callet-Bauchu E, Salles G, Sabatier L, Delic J, Gilson E. Changes in the expression of telomere maintenance genes suggest global telomere dysfunction in B-chronic lymphocytic leukemia. Blood 2008;111:2388–2391. [PubMed: 18077792]

Rudolph KL, Chang S, Lee HW, Blasco M, Gottlieb GJ, Greider C, DePinho RA. Longevity, stress response, and cancer in aging telomerase-deficient mice. Cell 1999;96:701–712. [PubMed: 10089885]

Rudolph KL, Millard M, Bosenberg MW, DePinho RA. Telomere dysfunction and evolution of intestinal carcinoma in mice and humans. Nat Genet 2001;28:155–159. [PubMed: 11381263]

Sarin KY, Cheung P, Gilison D, Lee E, Tennen RI, Wang E, Artandi MK, Oro AE, Artandi SE. Conditional telomerase induction causes proliferation of hair follicle stem cells. Nature 2005;436:1048–1052. [PubMed: 16107853]

Schrader M, Muller M, Schulze W, Heicappell R, Krause H, Straub B, Miller K. Quantification of telomerase activity, porphobilinogen deaminase and human telomerase reverse transcriptase mRNA in testicular tissue - new parameters for a molecular diagnostic classification of spermatogenesis disorders. Int J Androl 2002;25:34–44. [PubMed: 11869375]

Smogorzewska A, de Lange T. Different telomere damage signaling pathways in human and mouse cells. Embo J 2002;21:4338–4348. [PubMed: 12169636]

Tabori U, Nanda S, Druker H, Lees J, Malkin D. Younger age of cancer initiation is associated with shorter telomere length in Li-Fraumeni syndrome. Cancer Res 2007;67:1415–1418. [PubMed: 17308077]

van Steensel B, Smogorzewska A, de Lange T. TRF2 protects human telomeres from end-to-end fusions. Cell 1998;92:401–413. [PubMed: 9476899]

Vega F, Cho-Vega JH, Lennon PA, Luthra MG, Bailey J, Breeden M, Jones D, Medeiros LJ, Luthra R. Splenic marginal zone lymphomas are characterized by loss of interstitial regions of chromosome 7q, 7q31.32 and 7q36.2 that include the protection of telomere 1 (POT1) and sonic hedgehog (SHH) genes. Br J Haematol. 2008

Wu L, Multani AS, He H, Cosme-Blanco W, Deng Y, Deng JM, Bachilo O, Pathak S, Tahara H, Bailey SM, et al. Pot1 deficiency initiates DNA damage checkpoint activation and aberrant homologous recombination at telomeres. Cell 2006;126:49–62. [PubMed: 16839876]

Xin H, Liu D, Wan M, Safari A, Kim H, Sun W, O'Connor MS, Songyang Z. TPP1 is a homologue of ciliate TEBP-beta and interacts with POT1 to recruit telomerase. Nature 2007;445:559–562. [PubMed: 17237767]

Ye JZ, Hockemeyer D, Krutchinsky AN, Loayza D, Hooper SM, Chait BT, de Lange T. POT1-interacting protein PIP1: a telomere length regulator that recruits POT1 to the TIN2/TRF1 complex. Genes Dev 2004;18:1649–1654. [PubMed: 15231715]

Zanaria E, Muscatelli F, Bardoni B, Strom TM, Guioli S, Guo W, Lalli E, Moser C, Walker AP, McCabe ER, et al. An unusual member of the nuclear hormone receptor superfamily responsible for X-linked adrenal hypoplasia congenita. Nature 1994;372:635–641. [PubMed: 7990953]

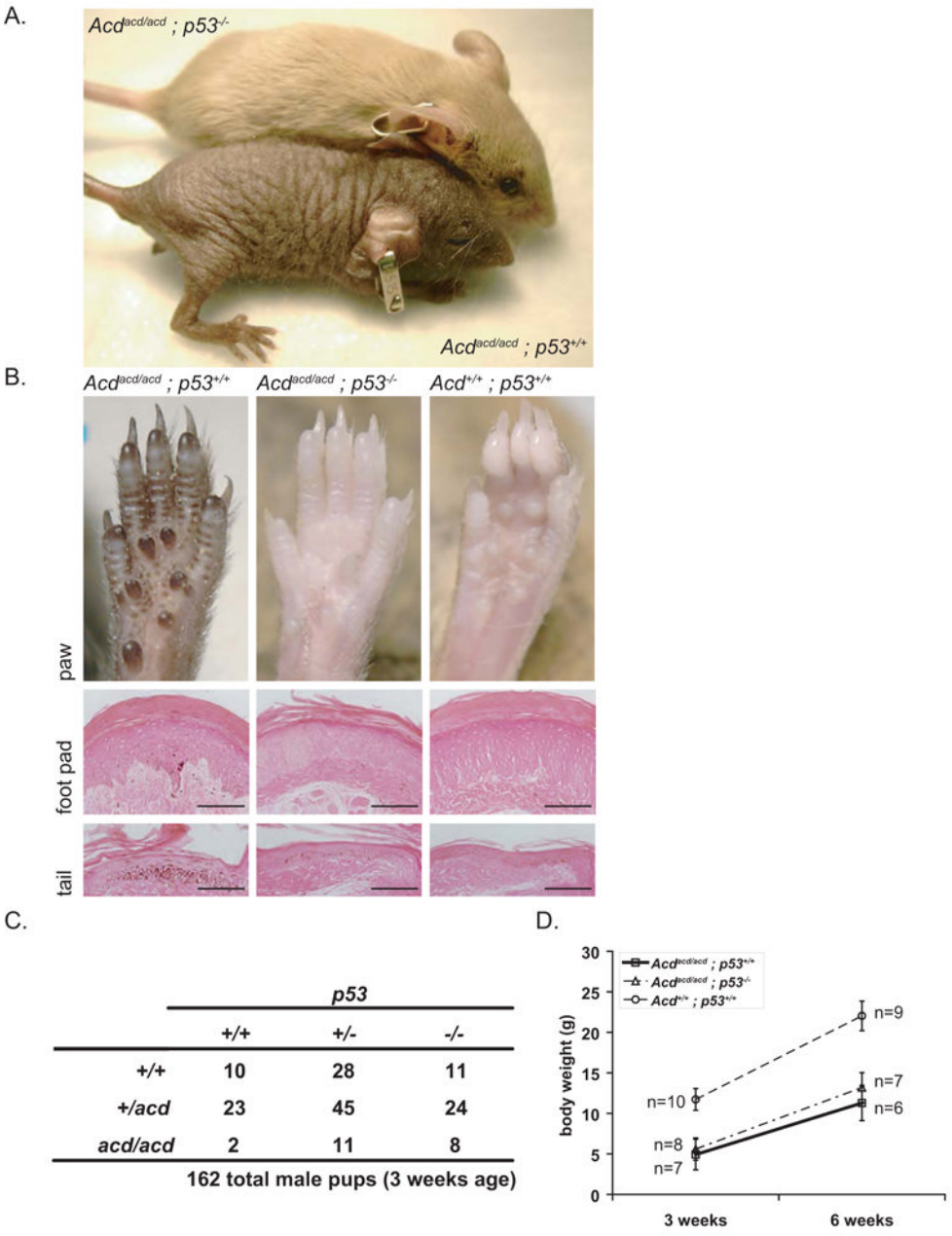

Figure 1. *p53* ablation reverses the macroscopic appearance of adrenocortical dysplasia mice and increases perinatal survival

(A) The macroscopic hyperpigmentation and fur phenotype of $Acd^{acd/acd}$ mice were completely rescued by *p53* ablation. Macroscopic appearance of 6 week old mice: $Acd^{acd/acd}$ $p53^{-/-}$ mice shown on top of the picture showed normal fur growth and completely lacked hyperpigmentation. As a comparison an $Acd^{acd/acd}$ $p53^{+/+}$ mouse is shown below.

(B) Hyperpigmentation is always present on the footpads of adrenocortical dysplasia mice. In $Acd^{acd/acd}$ $p53^{-/-}$ mice the hyperpigmentation completely disappeared at the macroscopic level. Eosin-stained sections showed a striking reduction of pigment in the epidermis and dermis of $Acd^{acd/acd}$ $p53^{-/-}$ mice. The same results are shown for tail skin sections (scale bars for foot pads 200μm, for tails 100μm).

(C) Genotype analysis of 162 male pups at weaning age shows an increased survival for $Acd^{acd/acd}$ $p53^{-/-}$ mice. $Acd^{acd/acd}$ mice with either the $p53^{+/-}$ or the $p53^{+/+}$ genotype were not observed in the expected ratio (p=0.03 and p=0.03 as compared to p=0.6 for $p53^{-/-}$, Chi-square test).

(D) $Acd^{acd/acd}$ $p53^{-/-}$ mice are still smaller than their $Acd^{+/+}$ $p53^{+/+}$ littermates ($p<10^{-7}$). Body weight did not differ from $Acd^{acd/acd}$ $p53^{+/+}$ mice (p=0.4 at 3 weeks and p=0.1 at 6 weeks, 1-way ANOVA and F-test, data shown as mean +/− SD). Post-weaning weight gain was comparable in both $Acd^{acd/acd}$ groups to their *wt* littermates..

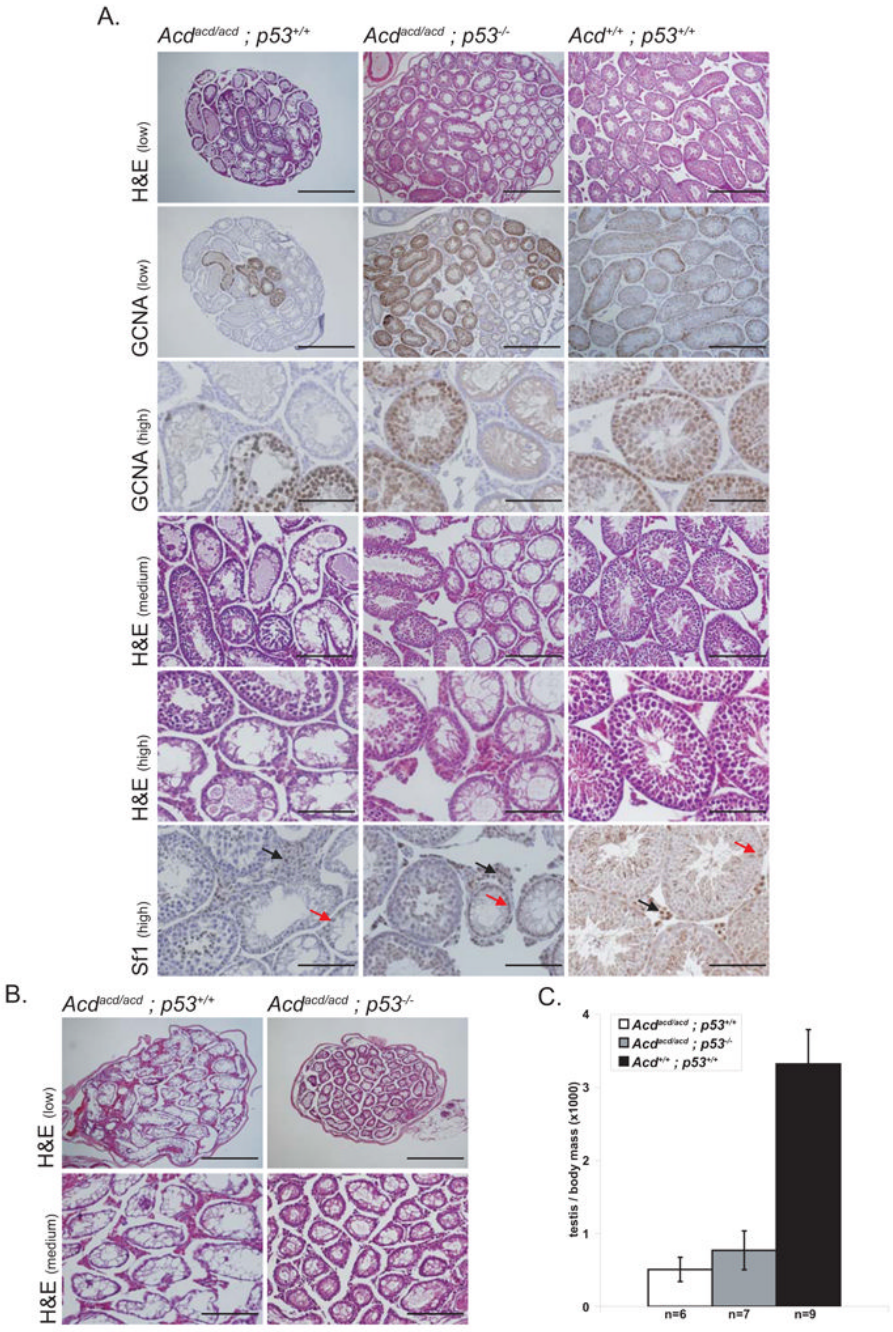

Figure 2. Loss of *p53* does not rescue spermatogenesis in $Acd^{acd/acd}$ testes. Testes of $Acd^{acd/acd}$ mice display focal or complete absence of germinal epithelia reminiscent of Sertoli-cell-only syndrome regardless of their genetic *p53* status

(A) Testes of $Acd^{acd/acd}$ $p53^{+/+}$ as well as $Acd^{acd/acd}$ $p53^{-/-}$ mice show focal spermatogenesis. Seminiferous tubules with an intact germinal cell epithelium harbored Gcna-positive germ cells. The Sf1-positive interstitial Leydig (black arrows) and Sertoli cell (red arrows) populations did not appear altered in either genotype compared to $Acd^{+/+}$ $p53^{+/+}$ littermates (scale bars for different levels of magnification: high 100μm, medium 200μm, low 400μm).

(B) Some *Acd*$^{acd/acd}$ *p53*$^{+/+}$ and *Acd*$^{acd/acd}$ *p53*$^{-/-}$ testes completely lack spermatogenesis and germ cells. Only empty seminiferous tubules were present in these testes (scale bars for different levels of magnification: medium 200μm, low 400μm).
(C) Testis weight relative to body weight is severely reduced in both *Acd*$^{acd/acd}$ *p53*$^{+/+}$ and *Acd*$^{acd/acd}$ *p53*$^{-/-}$ mice and therefore independent of their genetic *p53* status (*Acd*$^{+/+}$ *p53*$^{+/+}$ vs. *Acd*$^{acd/acd}$ *p53*$^{-/-}$ $p=1\times10^{-11}$, *Acd*$^{+/+}$ *p53*$^{+/+}$ vs. *Acd*$^{acd/acd}$ *p53*$^{+/+}$ $p=4\times10^{-12}$, *Acd*$^{acd/acd}$ *p53*$^{+/+}$ vs. *Acd*$^{acd/acd}$ *p53*$^{-/-}$, p=0.19, 1-way ANOVA and F-test, data shown as mean +/− SD)

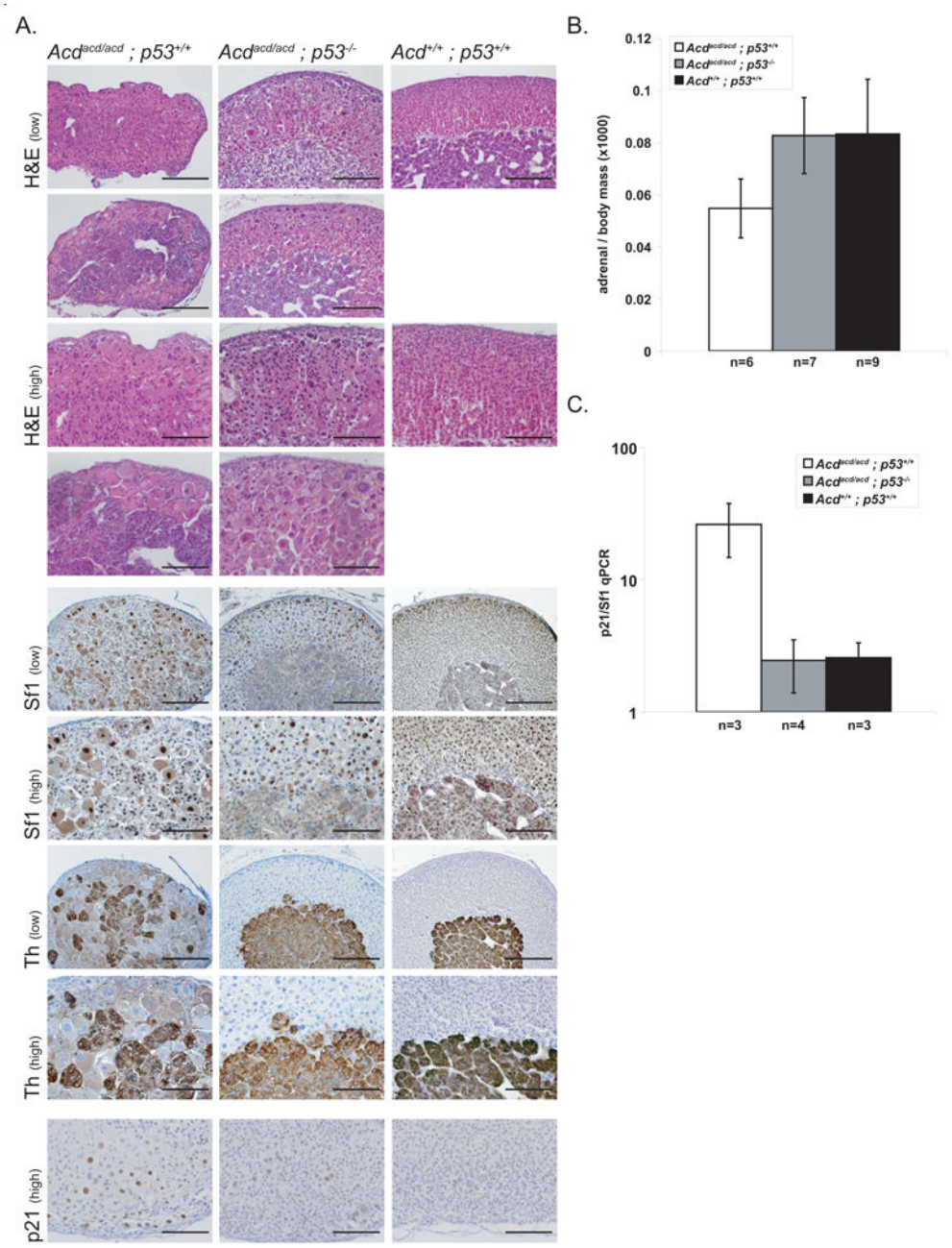

Figure 3. Adrenocortical architecture, weight and *p21* expression is normalized in adrenal cortex of $Acd^{acd/acd}$ $p53^{-/-}$ mice

(A) The adrenal cortex of $Acd^{acd/acd}$ mice appears highly disorganized and consists of scattered cells with a high grade of nuclear pleomorphy. This phenotype was partially rescued in $Acd^{acd/acd}$ $p53^{-/-}$ mice, where adrenal glands appeared more clearly zonated and organized, while increased nuclear size and pleomorphy partially persisted. This became obvious using differentiation markers for the adrenal cortex (Sf1, steroidogenic factor 1) and for the adrenal medulla (Th, tyrosine hydroxylase). Two examples of adrenal glands from $Acd^{acd/acd}$ $p53^{+/+}$ and $Acd^{acd/acd}$ $p53^{-/-}$ and, as a comparison, one *wt* ($Acd^{+/+}$ $p53^{+/+}$) adrenal, are shown. $Acd^{acd/acd}$ $p53^{+/+}$ adrenal cortices stained positive for p21, a downstream mediator of p53-

mediated senescence induction (scale bars for different levels of magnification: high 100μm, low 200μm).

(B) Relative adrenal gland weight is normalized in $Acd^{acd/acd}$ $p53^{-/-}$ mice. Adrenal glands from $Acd^{acd/acd}$ $p53^{+/+}$ animals were about 66% the relative weight of $Acd^{+/+}$ $p53^{+/+}$ adrenal glands ($Acd^{acd/acd}$ $p53^{+/+}$ vs. $Acd^{+/+}$ $p53^{+/+}$ p=0.008, $Acd^{acd/acd}$ $p53^{+/+}$ vs. $Acd^{acd/acd}$ $p53^{-/-}$ p=0.005, $Acd^{acd/acd}$ $p53^{-/-}$ vs. $Acd^{acd/acd}$ $p53^{+/+}$ p=0.95, 1-way ANOVA and F-test, data shown as mean +/− SD).

(C) In $Acd^{acd/acd}$ $p53^{+/+}$ mice telomere deprotection induces *p21* expression as a marker of senescence. Ablation of *p53* strikingly reduced *p21* expression ($Acd^{acd/acd}$ $p53^{+/+}$ vs. $Acd^{+/+}$ $p53^{+/+}$ p=0.02, $Acd^{acd/acd}$ $p53^{+/+}$ vs. $Acd^{acd/acd}$ $p53^{-/-}$ p=0.03, $Acd^{acd/acd}$ $p53^{-/-}$ vs. $Acd^{+/+}$ $p53^{+/+}$ p=0.99, 1-way ANOVA and F-test, data shown as mean +/− SD).

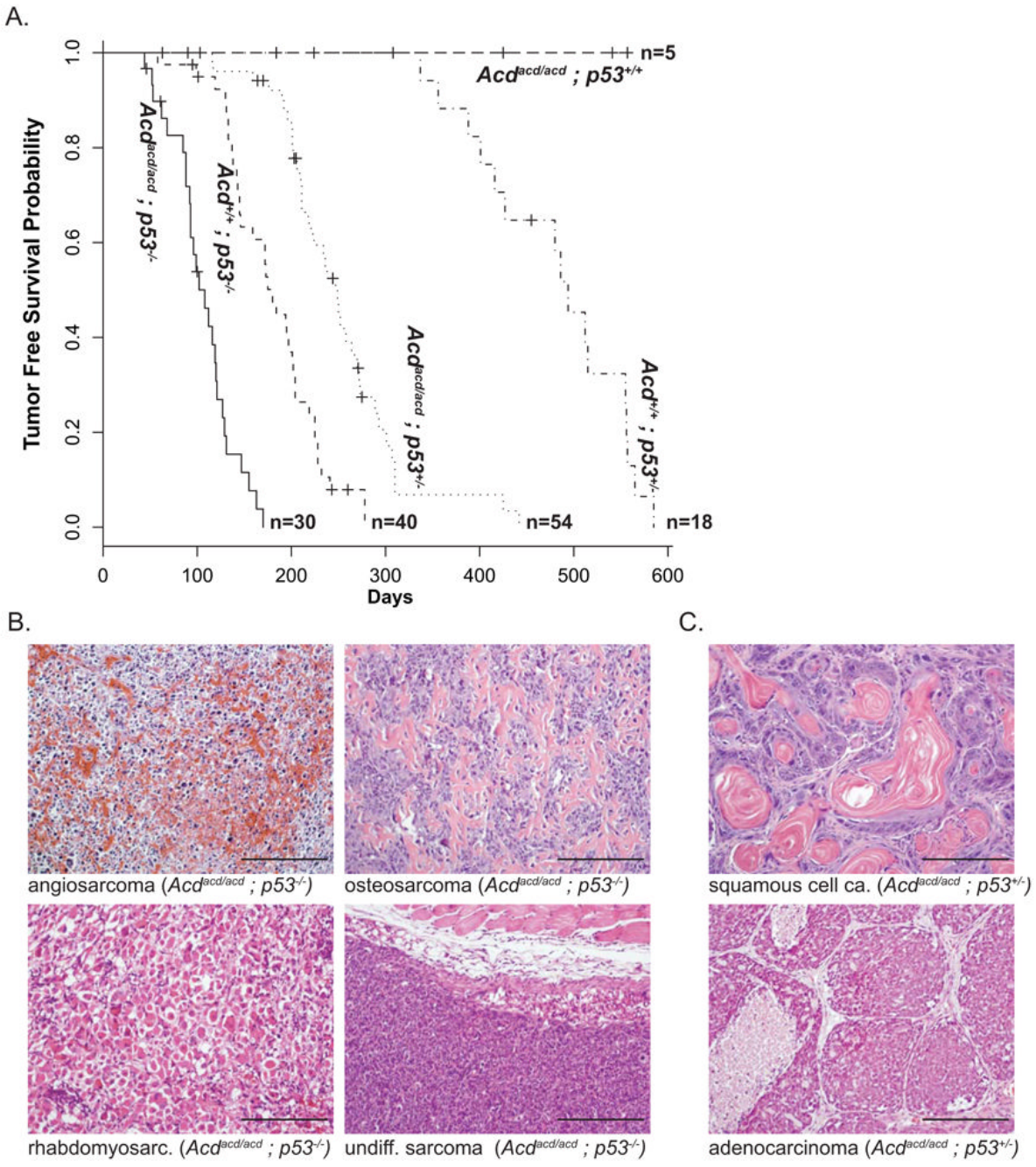

Figure 4. The $Acd^{acd/acd}$ genotype severely reduces tumor free survival in $p53^{-/-}$ and $p53^{+/-}$ mice

(A) Tumor free survival is shown for the different genotype cohorts as a Kaplan-Meier plot. On average in both groups, $p53^{-/-}$ and $p53^{+/-}$, mice with the $Acd^{acd/acd}$ genotype developed tumors in approximately half the amount of time compared to their $Acd^{+/+}$ littermates ($Acd^{acd/acd}$ $p53^{-/-}$ *vs.* $Acd^{+/+}$ $p53^{-/-}$ $p=2\times10^{-11}$ and $Acd^{acd/acd}$ *vs.* $p53^{+/-}$ $Acd^{+/+}$ $p53^{+/-}$ $p=2\times10^{-9}$, log-rank test). In contrast none of the $Acd^{acd/acd}$ $p53^{+/+}$ developed any tumors. **(B)** The main categories of solid tumors in $Acd^{acd/acd}$ $p53^{-/-}$ and $Acd^{+/+}$ $p53^{-/-}$ are of the sarcoma spectrum (examples of angiosarcoma, osteosarcoma, rhabdomyosarcoma and undifferentiated sarcoma are shown, scale bars 200μm)).

(C) In *Acd*$^{acd/acd}$ *p53*$^{+/-}$, but not *Acd*$^{+/+}$ *p53*$^{+/-}$, mainly carcinomas arose with a varying degree of squamous cell carcinoma or adenocarcinoma differentiation (scale bars 200μm).

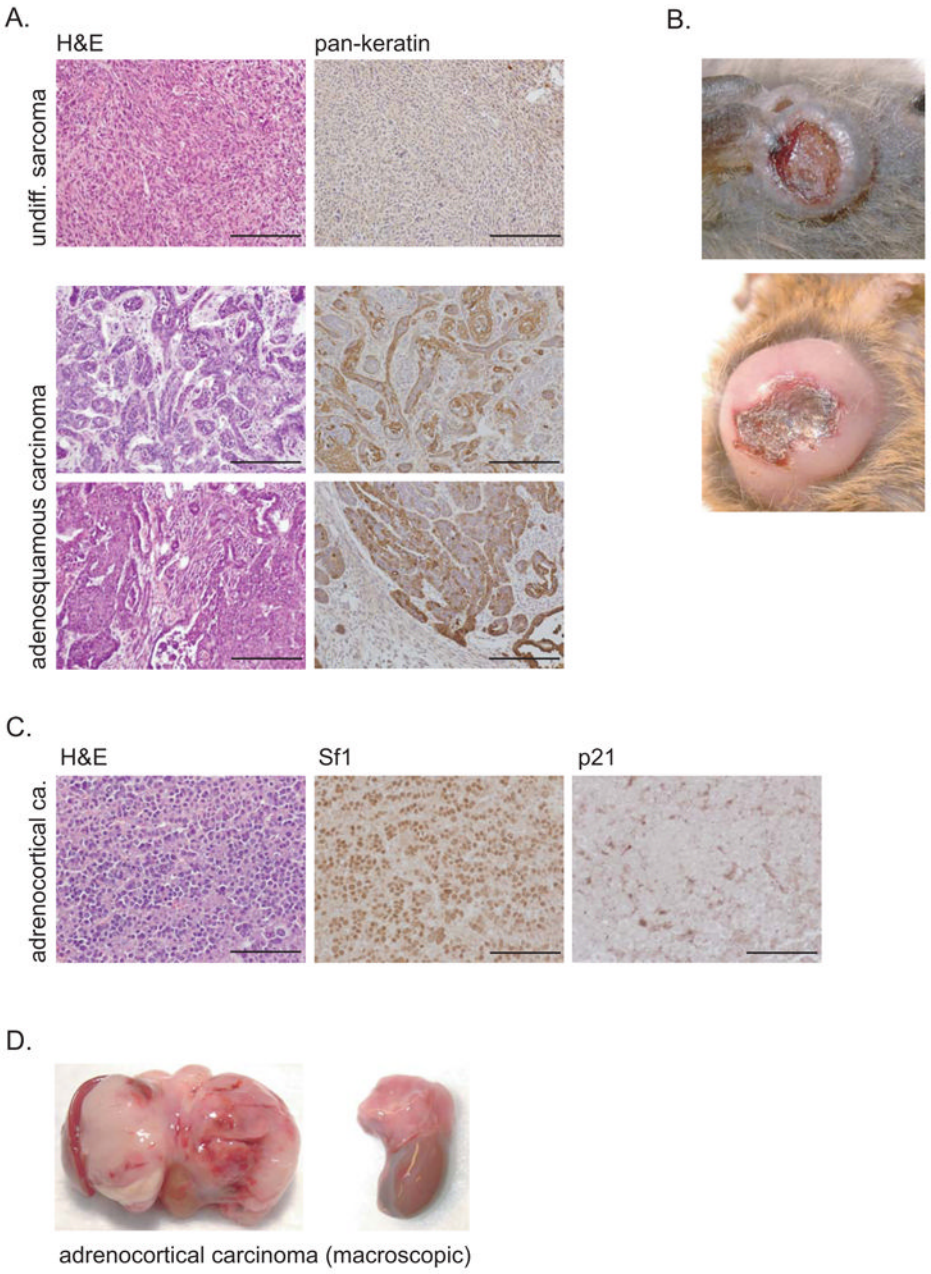

Figure 5. *Acd*$^{acd/acd}$ *p53*$^{+/-}$ mice predominantly develop carcinomas

(A) Some *Acd*$^{acd/acd}$ *p53*$^{+/-}$ carcinomas show an intermediate adenosquamous differentiation type with elements of squamous cell as well adenocarcinoma-like elements. Skin associated carcinomas stained highly positive for pankeratin (scale bars 200μm).

(B) Most carcinomas arise in the cutaneous or subcutaneous regions and typically show central necrosis.

(C) 5% of *Acd*$^{acd/acd}$ *p53*$^{+/-}$ develop adrenocortical cancers. Their origin could readily be identified by positive Sf1 staining. Adrenocortical cancers were p21 negative indicating that they evaded senescence (scale bars 100μm).

(D) Macroscopically, adrenocortical cancer expanded within the peritoneal cavity adhering to adjacent organs. Two examples of ACC from *Acd*$^{acd/acd}$ *p53*$^{+/-}$ mice are shown.

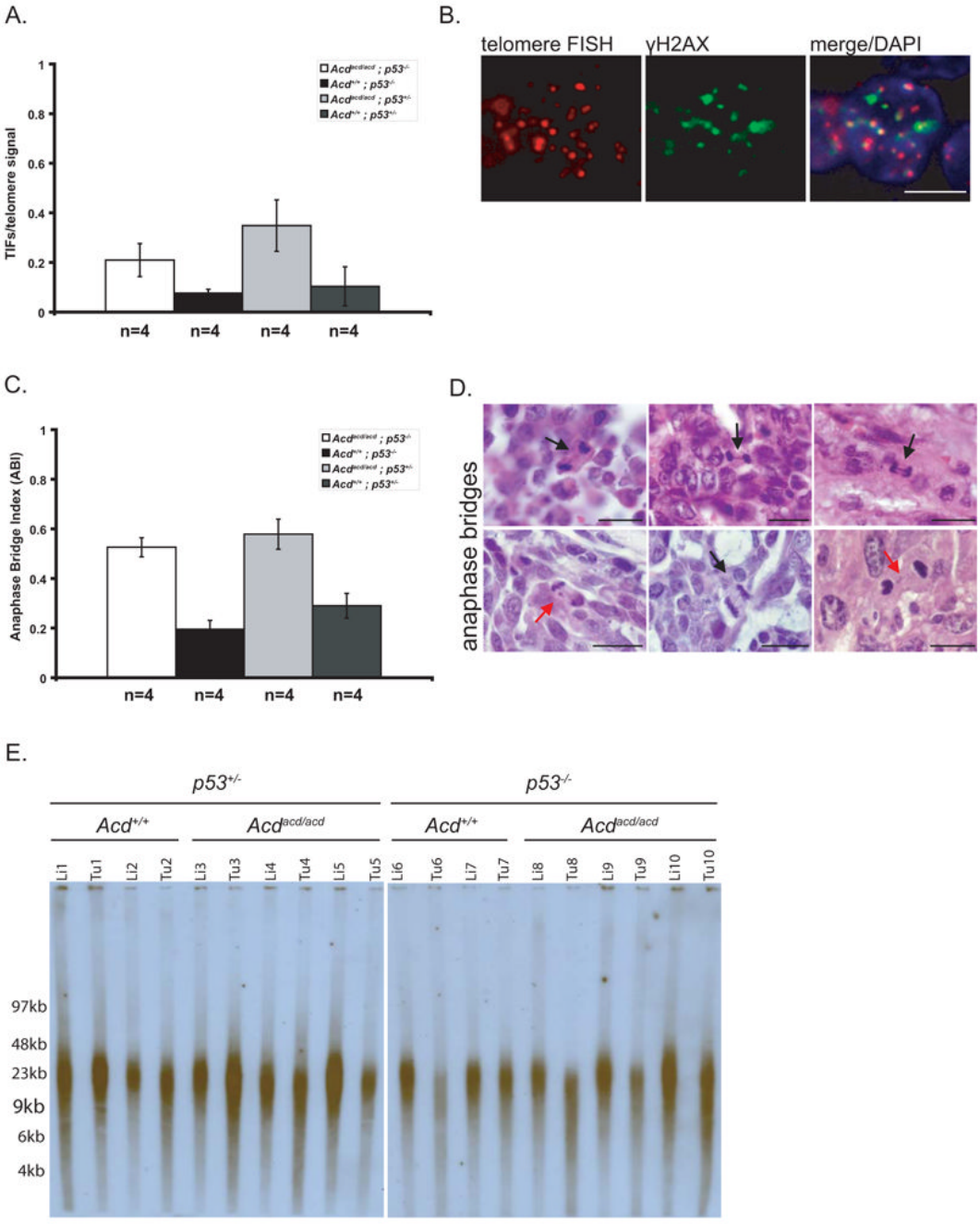

Figure 6. Tumors from *Acd*$^{acd/acd}$ mice exhibit hallmarks of genomic instability in the absence of significant telomere shortening

(A) *Acd*$^{acd/acd}$ tumors had significantly more telomere dysfunction induced foci (TIFs) per total telomere signals than *Acd*$^{+/+}$ tumors indicating that telomere decapping is evident in these neoplasms (p=0.047 for *Acd*$^{acd/acd}$ *p53*$^{-/-}$ vs. *Acd*$^{+/+}$ *p53*$^{-/-}$ tumors and p=0.002 for *Acd*$^{acd/acd}$ *p53*$^{+/-}$ vs. *Acd*$^{+/+}$ *p53*$^{+/-}$ tumors, 1-way ANOVA and F-test, data shown as mean +/− SD).

(B) Decapped telomeres recruit factors of the DNA surveillance machinery, such as γH2ax and form TIFs. TIFs, the classical co-localization of telomere FISH signal (red) and γH2ax immunohistochemistry (green), were observed in *Acd*$^{acd/acd}$ tumors (scale bars 5μm).

(C) Tumors from *Acd*$^{acd/acd}$ mice (*p53*$^{-/-}$ or *p53*$^{+/-}$) have a significantly increased anaphase bridge index (*Acd*$^{acd/acd}$ *p53*$^{-/-}$ *vs. Acd*$^{+/+}$ *p53*$^{-/-}$ p=5×10^{-5} and *Acd*$^{acd/acd}$ *vs. p53*$^{+/-}$ *Acd*$^{+/+}$ *p53*$^{+/-}$ p=0.001, 1-way ANOVA and F-test, data shown as mean +/− SD).
(D) Classical anaphase bridges, a morphological correlate of breakage-fusion-bridge cycles (BFBs), are present in tumors from *Acd*$^{acd/acd}$ mice (black arrows). In some instances chromosomal material (red arrows) appeared in between the two poles without a clear connection to either of the poles of the emerging daughter cells (scale bars 20μm).
(E) Telomere length as measured by TRF gel analysis. No clear differences between normal tissues (liver) of different genotypes were observed. The *Acd*$^{acd/acd}$ genotype itself did not lead to *in vivo* telomere length alteration in normal tissues. Some *Acd*$^{acd/acd}$ as well as *Acd*$^{+/+}$ tumors showed a moderate shortening of telomere length.

A.

Acd genotype	*p53* genotype	transitions	selected segments	runs	chromosomes	chromosomes with amplicons (deletions)
acd/acd	+/-	80	1	1	1	X
acd/acd	+/-	143	66	36	10	1,3,4,5,6,10,11,13,16, (19)
acd/acd	+/-	66	6	6	4	1,3,11, (10)
acd/acd	-/-	134	1	1	1	X
acd/acd	-/-	71	2	2	2	(6,14)
acd/acd	-/-	50	25	10	3	5,6,X
+/+	+/-	16	0	0	0	
+/+	+/-	34	7	6	2	(8,14)
+/+	-/-	33	9	1	1	9
+/+	-/-	25	0	0	0	
1-sided, (Wilcoxon) Rank-sum test		0.0048	0.23	0.064	0.041	

B.

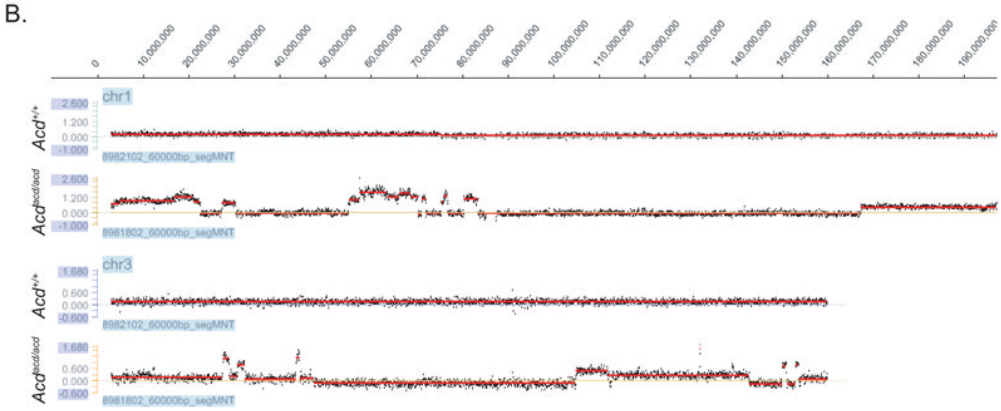

C.

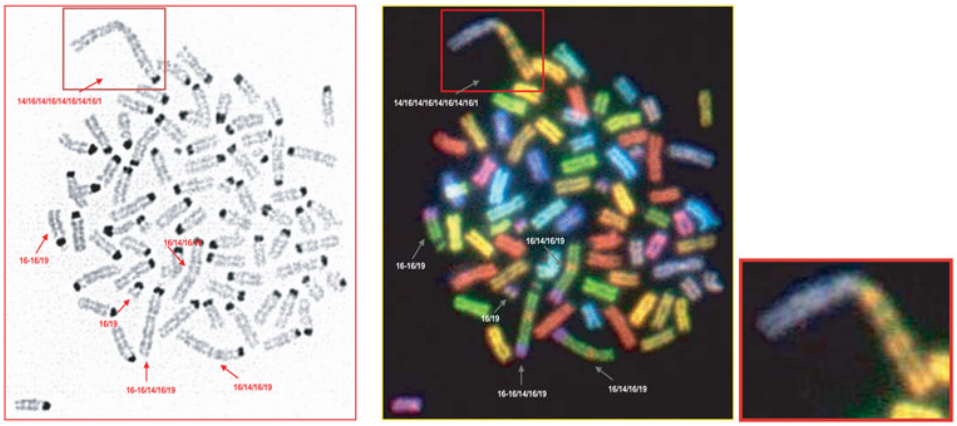

Figure 7. Telomere deprotection in tumors from *Acd*$^{acd/acd}$ mice leads to genomic and cytogenetic alterations as a consequence of breakage fusion bridge cycles

(A) Table summarizing characteristics of *Acd*$^{acd/acd}$ tumors as analyzed by CGH. *Acd*$^{acd/acd}$ tumors have significantly more transition points compared to *Acd*$^{+/+}$ tumors as would be expected with repeated BFBs and significantly more chromosomes exhibited copy number alterations.

(B) CGH example of tumor DNA normalized to same animal liver DNA. Multiple amplifications sometimes presenting in a stepwise manner of increasing amplification values on the same chromosome (e.g. chr. 1 and chr. 3 of two samples) were observed in *Acd*$^{acd/acd}$ (lower panel) but not in *Acd*$^{+/+}$ tumors (upper panel) (y-axis: $\log_2$ of tumor/liver).

(C) Spectral karyotyping of a cell line derived from a $Acd^{acd/acd}$ $p53^{-/-}$ rhabdomyosarcoma revealed genomic rearrangements in the form of hybrid chromosomes consisting of genomic stretches of original chromosome 16 and chromosome 19 (see magnification lower right)

Table 1

Distribution of tumor types in the different genotypes

Animals were autopsied at the time of either spontaneous death or visible tumor growth. Tumors from *Acd*$^{acd/acd}$ *p53*$^{+/-}$ mice had an overall higher occurrence of tumors of the carcinoma spectrum ($p=1\times10^{-14}$, 2-sided Fisher's Exact test). Carcinomas and sarcomas are broken down in distinct tumor diagnosis. Most of the *Acd*$^{acd/acd}$ *p53*$^{+/-}$ tumors were of a squamous cell carcinoma, adenocarcinoma or adenosquamous carcinoma differentiation type. All other tumor types fell into the typical spectrum of *p53*$^{-/-}$ tumors (i.e., sarcomas and lymphomas).

	acd/acd; p53−/−	***+/+; p53−/−***	***acd/acd; p53+/−***	***+/+; p53+/−***
sarcoma	**16 (47%)**	**18 (44%)**	**11 (26%)**	**9 (50%)**
angiosarcoma	*7 (21%)*	*12 (29%)*	*0 (0%)*	*0 (0%)*
rhabdomyosarcoma	*3 (9%)*	*1 (2%)*	*0 (0%)*	*0 (0%)*
osteosarcoma	*2 (6%)*	*0 (0%)*	*4 (10%)*	*6 (33%)*
MFH	*1 (3%)*	*0 (0%)*	*2 (5%)*	*0 (0%)*
fibrosarcoma	*0 (0%)*	*2 (5%)*	*0 (0%)*	*1 (6%)*
chondrosarcoma	*0 (0%)*	*0 (0%)*	*1 (2%)*	*0 (0%)*
undiff. sarcoma	*3 (9%)*	*3 (7%)*	*4 (10%)*	*2 (11%)*
carcinoma	**2 (6%)**	**0 (0%)**	**27 (64%)**	**1 (6%)**
adenocarcinoma	*1 (3%)*	*0 (0%)*	*8 (19%)*	*0 (0%)*
adenosquamous ca.	*0 (0%)*	*0 (0%)*	*6 (14%)*	*0 (0%)*
SCC	*0 (0%)*	*0 (0%)*	*7 (17%)*	*1 (6%)*
HCC	*1 (3%)*	*0 (0%)*	*1 (2%)*	*0 (0%)*
ACC	*0 (0%)*	*0 (0%)*	*2 (5%)*	*0 (0%)*
undiff. carcinoma	*0 (0%)*	*0 (0%)*	*3 (7%)*	*0 (0%)*
lymphoma	**13 (38%)**	**19 (46%)**	**3 (7%)**	**7 (39%)**
Germ cell	**1 (3%)**	**1 (2%)**	**0 (0%)**	**1 (6%)**
Brain	**1 (3%)**	**2 (5%)**	**0 (0%)**	**0 (0%)**
undiff./not class.	**1 (3%)**	**1 (2%)**	**1 (2%)**	**0 (0%)**
Total	**34 (100%)**	**41 (100%)**	**42 (100%)**	**18 (100%)**